



**HAL**  
open science

## Looking into the dynamics of molecular crystals of ibuprofen and terephthalic acid using $^{17}\text{O}$ and $^2\text{H}$ NMR analyses

Chia-Hsin Chen, Ieva Goldberga, Philippe Gaveau, Sébastien Mittelette, Jessica Špačková, Chuck Mullen, Ivan Petit, Thomas-Xavier Métro, Bruno Alonso, Christel Gervais, et al.

### ► To cite this version:

Chia-Hsin Chen, Ieva Goldberga, Philippe Gaveau, Sébastien Mittelette, Jessica Špačková, et al.. Looking into the dynamics of molecular crystals of ibuprofen and terephthalic acid using  $^{17}\text{O}$  and  $^2\text{H}$  NMR analyses. *Magnetic Resonance in Chemistry*, 2021, 59 (9-10), pp.975-990. 10.1002/mrc.5141 . hal-03205685v2

HAL Id: hal-03205685

<https://hal.science/hal-03205685v2>

Submitted on 16 May 2024









**HAL** is a multi-disciplinary open access archive for the deposit and dissemination of scientific research documents, whether they are published or not. The documents may come from teaching and research institutions in France or abroad, or from public or private research centers.

L'archive ouverte pluridisciplinaire **HAL**, est destinée au dépôt et à la diffusion de documents scientifiques de niveau recherche, publiés ou non, émanant des établissements d'enseignement et de recherche français ou étrangers, des laboratoires publics ou privés.



Distributed under a Creative Commons Attribution - NonCommercial - NoDerivatives 4.0 International License

# Looking into the dynamics of molecular crystals of ibuprofen and terephthalic acid using $^{17}\text{O}$ and $^2\text{H}$ nuclear magnetic resonance analyses

Chia-Hsin Chen<sup>1</sup>  | Ieva Goldberga<sup>1</sup>  | Philippe Gaveau<sup>1</sup> | Sébastien Mittlelette<sup>1</sup>  | Jessica Špačková<sup>1</sup>  | Chuck Mullen<sup>2</sup> | Ivan Petit<sup>3</sup> | Thomas-Xavier Métro<sup>4</sup>  | Bruno Alonso<sup>1</sup>  | Christel Gervais<sup>3</sup>  | Danielle Laurencin<sup>1</sup> 

<sup>1</sup>ICGM, Univ Montpellier, CNRS, ENSCM, Montpellier, France

<sup>2</sup>PhoenixNMR, Loveland, Colorado, USA

<sup>3</sup>Laboratoire de Chimie de la Matière Condensée de Paris (LCMCP), UMR 7574, Sorbonne Université, CNRS, Paris, France

<sup>4</sup>IBMM, Univ Montpellier, CNRS, ENSCM, Montpellier, France

## Correspondence

Danielle Laurencin, ICGM, Univ Montpellier, CNRS, ENSCM, Montpellier, France.

Email: danielle.laurencin@umontpellier.fr

## Funding information

GENCI-IDRIS, Grant/Award Number: 097535; Horizon 2020, Grant/Award Number: 772204

## Abstract

Oxygen-17 and deuterium are two quadrupolar nuclei that are of interest for studying the structure and dynamics of materials by solid-state nuclear magnetic resonance (NMR). Here,  $^{17}\text{O}$  and  $^2\text{H}$  NMR analyses of crystalline ibuprofen and terephthalic acid are reported. First, improved  $^{17}\text{O}$ -labelling protocols of these molecules are described using mechanochemistry. Then, dynamics occurring around the carboxylic groups of ibuprofen are studied considering variable temperature  $^{17}\text{O}$  and  $^2\text{H}$  NMR data, as well as computational modeling (including molecular dynamics simulations). More specifically, motions related to the concerted double proton jump and the  $180^\circ$  flip of the H-bonded ( $-\text{COOH}$ )<sub>2</sub> unit in the crystal structure were looked into, and it was found that the merging of the C=O and C–OH  $^{17}\text{O}$  resonances at high temperatures cannot be explained by the sole presence of one of these motions. Lastly, preliminary experiments were performed with a  $^2\text{H}$ – $^{17}\text{O}$  diplexer connected to the probe. Such configurations can allow, among others,  $^2\text{H}$  and  $^{17}\text{O}$  NMR spectra to be recorded at different temperatures without needing to tune or to change probe configurations. Overall, this work offers a few leads which could be of use in future studies of other materials using  $^{17}\text{O}$  and  $^2\text{H}$  NMR.

## KEYWORDS

solid state NMR, deuterium, molecular crystals, oxygen-17, dynamics, GIPAW, diplexer, molecular dynamics, tautomerism, hydrogen bonding

Chia-Hsin Chen and Ieva Goldberga contributed equally to this work.

This is an open access article under the terms of the Creative Commons Attribution-NonCommercial-NoDerivs License, which permits use and distribution in any medium, provided the original work is properly cited, the use is non-commercial and no modifications or adaptations are made.

© 2021 The Authors. *Magnetic Resonance in Chemistry* published by John Wiley & Sons Ltd.

## 1 | INTRODUCTION

The potential of solid-state nuclear magnetic resonance (NMR) techniques for helping study the structure and reactivity of complex (bio)molecular and materials systems has significantly increased in recent years, thanks to numerous developments made in terms of instrumentation (e.g., ultrahigh magnetic fields and ultrafast magic angle spinning—MAS—probes),<sup>[1–3]</sup> pulse sequence developments (e.g., <sup>1</sup>H-detected sequences, ultrawide line, and broadband acquisition methods),<sup>[2,4–8]</sup> more efficient and/or selective isotopic enrichment approaches,<sup>[9–12]</sup> and Dynamic Nuclear Polarization (DNP).<sup>[13,14]</sup> Studies on challenging quadrupolar nuclei of low receptivity are increasingly being reported, including for some of the most « exotic » ones,<sup>[15,16]</sup> like <sup>43</sup>Ca, <sup>61</sup>Ni, <sup>87</sup>Sr and <sup>90</sup>Zr, just to name a few. Moreover, investigations aiming at understanding the dynamics occurring at different timescales within (bio)molecular and materials systems are seen as highly important, not only because of the impact they can have on the NMR spectra and their acquisition conditions, but also and more importantly because of the insight they can provide on the properties of a given (bio)molecule or material.<sup>[17–21]</sup>

When it comes to studying dynamics in materials involving small organic molecules, <sup>2</sup>H and <sup>17</sup>O are both attractive quadrupolar nuclei.<sup>[22–29]</sup> This is notably true in crystals composed of molecules with carboxylic acid groups associated as dimers. Indeed, the dynamics of protons « hopping » between the H-bonded C=O and C–OH groups have been the object of much research, including using <sup>2</sup>H and <sup>17</sup>O magnetic resonance techniques.<sup>[24,30–32]</sup> Among recent <sup>2</sup>H studies, Schmidt and Sebastiani's work showed by *ab initio* calculations that the <sup>2</sup>H quadrupolar parameters in strongly H-bonded systems could not be directly transposed into structural data such as bond lengths, due to the importance of non-linear effects and collective motions.<sup>[32]</sup> Regarding <sup>17</sup>O, Wu and co-workers' investigations are worth highlighting: they demonstrated by using variable temperature <sup>17</sup>O NMR analyses that it is possible to study the concerted double-proton jumping, and estimate the energy asymmetry between the two H-bonded tautomers experimentally.<sup>[24]</sup> More generally speaking, when looking at the available literature, it appears that the information arising from <sup>2</sup>H

and <sup>17</sup>O NMR analyses can potentially provide complementary information on the dynamic processes taking place within carboxylic acid dimers.

Considering the above context, the purpose of this article is to expand the possibilities for studying dynamics within molecular crystals by <sup>2</sup>H and <sup>17</sup>O NMR. Our studies were performed on two molecules: terephthalic acid and ibuprofen. Because of the very low natural abundance of both isotopes (Table 1), analyses were performed on enriched samples. First, improved <sup>17</sup>O-labelling protocols based on mechanochemistry<sup>[33]</sup> are described for both molecules. They were used to produce two doubly labelled compounds (enriched in <sup>2</sup>H and <sup>17</sup>O), referred to as **D-TA\*** and **D-IBU\***, which were isolated as molecular crystals (Scheme 1). Second, a variable temperature <sup>17</sup>O MAS NMR study of **D-IBU\*** is presented. The <sup>17</sup>O NMR spectra are discussed using complementary computational modelling studies, including molecular dynamics simulations and *ab initio* calculations of NMR parameters. Lastly, preliminary NMR investigations involving a <sup>2</sup>H–<sup>17</sup>O diplexer connected to the NMR probe are presented. This system was used in the case of **D-TA\***, enabling some of the <sup>2</sup>H and <sup>17</sup>O NMR experiments to be performed at different temperatures in a back-to-back fashion with no need to retune the probe. This configuration is not standard considering the very similar Larmor frequencies of both nuclei (Table 1). Overall, the results presented in this manuscript will be of interest for future investigations of structure and dynamics using <sup>17</sup>O and/or <sup>2</sup>H NMR.

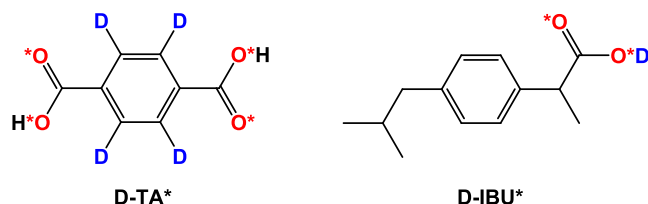
## 2 | EXPERIMENTAL SECTION

### 2.1 | Isotopic labelling procedures for terephthalic acid and ibuprofen

The following reagents were used as received: ibuprofen (C<sub>13</sub>H<sub>18</sub>O<sub>2</sub>, Sigma Aldrich, ≥98% purity, racemic form, noted here IBU), terephthalic acid (C<sub>8</sub>H<sub>6</sub>O<sub>4</sub>, Janssen Chemicals, 98% purity, noted here TA), and deuterated terephthalic acid (C<sub>8</sub>D<sub>4</sub>H<sub>2</sub>O<sub>4</sub>, with full deuteration on the aromatic cycle, 98% purity, Cambridge Isotope Laboratories, noted here D-TA) 1,1'-carbonyldiimidazole (C<sub>7</sub>H<sub>6</sub>N<sub>4</sub>O, TCI, >97% purity, noted here CDI).

	<sup>1</sup> H	<sup>2</sup> H	<sup>17</sup> O
Spin	1/2	1	5/2
Natural abundance	99.98%	0.015%	0.037%
Larmor frequency $\nu_0$ (MHz) at 14.1 T	600.1	92.1	81.4
Quadrupole moment $Q$ ( $\times 10^{-30}$ m <sup>2</sup> ) <sup>[34]</sup>	/	2.86	–25.58

TABLE 1 Nuclear spin properties of <sup>1</sup>H, <sup>2</sup>H and <sup>17</sup>O



**SCHEME 1** Structures of the doubly labelled  $^{17}\text{O}$  and  $^2\text{H}$  molecules: terephthalic acid (left) and ibuprofen (right). The  $^{17}\text{O}$ -labelling procedure by mechanochemistry leads to the predominant labelling of one oxygen per carboxylic group, but with both O atoms having the same probability to be enriched (which is why they are both highlighted in red)

$^{18}\text{O}$ -labelled water was purchased from Eurisotop (isotopic composition indicated in the certificate of analysis: 97.1%  $^{18}\text{O}$ , 1.1%  $^{17}\text{O}$  and 1.8%  $^{16}\text{O}$ ) or CortecNet (isotopic composition indicated in the certificate of analysis: 99.3%  $^{18}\text{O}$ , 0.2%  $^{17}\text{O}$  and 0.5%  $^{16}\text{O}$ ), and used for the optimisation of the enrichment protocols of terephthalic acid and ibuprofen, respectively, as detailed below.

$^{17}\text{O}$ -labelled water was purchased from CortecNet. The isotopic composition indicated in the certificate of analysis was 8.6%  $^{18}\text{O}$ , 90.4%  $^{17}\text{O}$  and 1.0%  $^{16}\text{O}$  for the  $\sim 90\%$   $^{17}\text{O}$ -enriched  $\text{H}_2\text{O}$ , and 43%  $^{18}\text{O}$ , 41%  $^{17}\text{O}$  and 16%  $^{16}\text{O}$  for the  $\sim 40\%$   $^{17}\text{O}$   $\text{H}_2\text{O}$ .

$\text{D}_2\text{O}$  (> 99.96%, CAS 7789-20-0) was purchased from Sigma-Aldrich.

Reagent grade solvents were used in all purification protocols.

### 2.1.1 | $^{17}\text{O}$ -enrichment of terephthalic acid and deuterated terephthalic acid by mechanochemistry

The enrichment procedure was first optimised using  $^{18}\text{O}$ -enriched water, due to its lower cost compared to  $^{17}\text{O}$ -enriched water. Terephthalic acid (50 mg, 0.30 mmol and 1.0 eq) and CDI (107 mg, 0.66 mmol and 2.2 eq) were introduced in a stainless-steel grinding jar (10 ml inner volume) with two stainless steel balls (10 mm diameter). The jar was closed and subjected to grinding for 60 min in the MM400 mixer mill operating at 25 Hz.  $^{18}\text{O}$ -labelled water (16  $\mu\text{l}$ , 0.88 mmol and  $\sim 3$  eq) was then introduced in the jar, and the mixture was subjected to further grinding for 60 min at 25 Hz. To help recover the product, non-labelled water (1 ml) was introduced in the jar, and the medium was subjected to grinding for 2 min at 25 Hz. Then, it was transferred to an Erlenmeyer flask (together with  $2 \times 1$  ml of non-labelled water, used here to rinse the grinding jar). The medium was acidified to pH  $\sim 1$  by adding a few drops of concentrated HCl (6 mol.L $^{-1}$  aqueous solution,  $\sim 15$  drops). The white

precipitate was immediately filtered on a glass frit, washed with  $4 \times 0.5$  ml of a 1 mol.L $^{-1}$  aqueous solution of HCl, and then with 0.5 ml of ultrapure water. The recovered solid was dried overnight under vacuum. Average yield ( $n = 3$ ,  $n$  representing the number of independent labelling experiments performed): 43 mg, 86%. Average  $^{18}\text{O}$ -enrichment level per oxygen, as determined by MS ( $n = 3$ ) =  $46 \pm 1\%$ .

For the preparation of the  $^{17}\text{O}$ - and  $^2\text{H}$ -enriched phase (noted **D-TA\***),  $\text{D}_4$ -terephthalic acid was used as a precursor, and the  $^{17}\text{O}$ -labelling step was performed following the optimised  $^{18}\text{O}$ -enrichment protocol described above using  $\sim 40\%$   $^{17}\text{O}$ -labelled water for the hydrolysis step instead (yield: 42 mg; average  $^{17}\text{O}$ -enrichment level per oxygen, as determined by MS =  $20 \pm 1\%$ ). The  $^1\text{H}$  and  $^{13}\text{C}$  solution NMR spectra, ESI-MS spectrum and X-ray powder diffraction (XRD) powder pattern of **D-TA\*** are shown in supporting information (Figures S1–S3).

### 2.1.2 | $^{17}\text{O}$ -enrichment of ibuprofen by mechanochemistry

The enrichment procedure was first optimised using  $^{18}\text{O}$ -enriched water, due to its lower cost compared to  $^{17}\text{O}$ -enriched water. Ibuprofen (120 mg, 0.58 mmol and 1.0 eq) and CDI (103 mg, 0.64 mmol and 1.1 eq) were introduced into a Retsch MM400 stainless steel grinding jar (10 ml inner volume) containing two stainless steel balls (10 mm diameter). The jar was closed and subjected to grinding for 30 min in the MM400 mixer mill operating at 25 Hz.  $^{18}\text{O}$ -labelled water (99.3%, 16  $\mu\text{l}$ , 0.87 mmol and 1.5 eq) was then added into the jar, and the mixture was subjected to further grinding for 30 min at 25 Hz. To help recover the product, non-labelled water (2 ml) was added into the jar, and the content was subjected to grinding for 2 min at 25 Hz. Then, the medium was transferred to a beaker (together with a sufficient amount of non-labelled water [8 ml] used here to rinse the jar). The medium was then acidified to pH  $\sim 1$  with an aqueous solution of HCl (6 mol.L $^{-1}$ ,  $\sim 18$  drops). The white precipitate was filtered on a glass frit, and  $2 \times 5$  ml of non-labelled water was used to help recover the rest of the product from the beaker. The product was washed with a 1 mol.L $^{-1}$  aqueous solution of HCl and ultrapure water ( $3 \times 1$  ml of each), and then dried under vacuum. Average synthetic yield ( $n = 3$ ): 89 mg, 75%. Average  $^{18}\text{O}$ -enrichment level per oxygen, as determined by MS ( $n = 3$ ):  $45 \pm 2\%$ .

For the preparation of the  $^{17}\text{O}$ -enriched phase (noted **IBU\***), the  $^{17}\text{O}$ -labelling step was first performed following the optimised  $^{18}\text{O}$ -enrichment protocol described above, but using  $\sim 90\%$   $^{17}\text{O}$ -labelled water (16  $\mu\text{l}$  and 1.5 eq.) for the hydrolysis step. Synthetic yield: 96 mg,

79%. Average  $^{17}\text{O}$ -enrichment level per oxygen, as determined by MS =  $36 \pm 2\%$  (average of five measurements). The  $^1\text{H}$  and  $^{13}\text{C}$  solution NMR spectra, ESI-MS spectrum, and XRD powder pattern of IBU\* are shown in supporting information (Figures S4–S6).

### 2.1.3 | $^2\text{H}$ -enrichment of $^{17}\text{O}$ -labelled ibuprofen

The deuteration step was performed by mixing 59.4 mg of  $^{17}\text{O}$ -labelled ibuprofen (IBU\*) with 0.5 ml of  $\text{D}_2\text{O}$  ( $\sim 95$  eq) in a 1.0-ml Eppendorf tube. The sample was sonicated for 1 min to ensure good mixing of the reagents. The mixture was then left for 3 days on a laboratory rocker shaker (Stuart SSL4—Rocker), with 70 oscillations per minute at room temperature. The mixture was spun down at 20,000 rpm for 15 min, and the excess water was discarded. The sample was then freeze-dried under vacuum for 6 h to remove the rest of the water. Synthetic yield: 56.4 mg, 95%. The IR and XRD powder patterns of the doubly labelled product **D-IBU\*** can be found in supporting information (Figures S4 and S8). A similar  $^2\text{H}$ -labelling protocol was also applied to non-labelled ibuprofen, on which complementary  $^2\text{H}$  MAS NMR experiments were performed.

### 2.2 | General characterisation protocols of the enriched compounds

Infrared (IR) spectra were recorded on a Perkin Elmer Spectrum 2 FT-IR instrument. The attenuated total reflectance (ATR) measurement mode was used (diamond crystal), and measurements were performed in the 400 to 4000  $\text{cm}^{-1}$  range.

Powder XRD analyses were carried out on an X'Pert MPD diffractometer using  $\text{Cu K}\alpha_1$  radiation ( $\lambda = 1.5406 \text{ \AA}$ ) with the operation voltage and current maintained at 40 kV and 25 mA, respectively. Diffractograms were recorded between  $5^\circ$  and  $50^\circ$  (or  $60^\circ$ ) in  $2\theta$ , with a step size of  $0.017^\circ$ , and a time per step of 20 to 40 s.

Mass spectrometry (MS) analyses were performed on a Waters Synapt G2-S apparatus, using electrospray ionisation in negative mode in a range of 50–1500 Da. Capillary and cone voltages were set to 3000 and 30 V, respectively. The source temperature was  $100^\circ\text{C}$ , and the desolvation temperature was set to  $250^\circ\text{C}$ . Data were processed by MassLynxV4.1 software. For each product, a solution was prepared (in ethanol or DMSO, depending on the solubility), which was analysed five times by ESI-MS.

$^1\text{H}$  and  $^{13}\text{C}$  solution NMR spectra were recorded on an Avance III Bruker 600 MHz spectrometer equipped with a TCI Prodigy cryoprobe, using  $\text{DMSO-}d_6$  as a solvent. Chemical shifts were referenced to the residual solvent peaks at 2.50 ppm ( $^1\text{H}$  NMR spectra) and 39.52 ppm ( $^{13}\text{C}$  NMR spectra).

The melting points of ibuprofen (IBU) and its enriched counterparts (IBU\* and D-IBU\*) were measured on a Büchi B-540 Melting Point Apparatus. Samples were heated up to  $70^\circ\text{C}$ , and then with a ramp of  $1^\circ\text{C min}^{-1}$  up to  $80^\circ\text{C}$ . All measurements were done in triplicate ( $n = 3$ ) and are reported in Table S1. The  $^2\text{H}$  and  $^{17}\text{O}$  NMR spectra of melted D-IBU\* are shown in Figure S9.

### 2.3 | Solid-state NMR experiments

Solid-state NMR experiments were performed on a Varian VNMRS 600 MHz (14.1 T) spectrometer, using, in the vast majority of cases, a PhoenixNMR HXY probe equipped with a 3.2 mm probe head. The PhoenixNMR probe was tuned to  $^1\text{H}$  (599.82 MHz),  $^2\text{H}$  (92.07 MHz) and  $^{17}\text{O}$  (81.33 MHz), using a  $^2\text{H}$ - $^{17}\text{O}$  diplexer. Conversion from multiple to single port tuning required a 'special' tuning plug-in and diplexer built specifically for  $^2\text{H}$  and  $^{17}\text{O}$ . Radio-frequency (RF) for  $^2\text{H}$  and  $^{17}\text{O}$  from the NMR console goes through a PhoenixNMR diplexer that provides  $>100$  dBc isolation and then into the probe on a single channel. The PhoenixNMR probe is adapted to provide an over-coupled double resonant structure for the  $^2\text{H}$  and  $^{17}\text{O}$  frequencies, which in conjunction with the diplexer can allow the observation of one channel while irradiating on the other. Spectra were recorded under static or MAS conditions, with spinning speeds ranging from 5 to 18 kHz, depending on the sample. In the case of the  $^2\text{H}$ -enriched ibuprofen (not labelled in  $^{17}\text{O}$ ), complementary  $^2\text{H}$  MAS NMR experiments were performed on a Varian T3 HX probe, tuned to  $^2\text{H}$  and  $^1\text{H}$ , and spinning at 5 kHz.

$^{17}\text{O}$  NMR experiments were recorded using DFS (double frequency sweep) pulse sequence with a rotor-synchronised echo of one rotor period. The parameters were as follows: DFS pulse of 500  $\mu\text{s}$  ( $\nu_{\text{RF}}[^{17}\text{O}] \sim 7.4$  kHz), with a sweep between 70 and 200 kHz, followed by a  $^{17}\text{O}$  excitation pulse of 2  $\mu\text{s}$ , echo delay of 55.55  $\mu\text{s}$ , and a  $\pi$  pulse of 4  $\mu\text{s}$ . All experiments were performed with a MAS frequency of 18 kHz and recycle delay of 0.5 s, and the number of transients acquired was 2400 for D-TA\* and 4000 for D-IBU\*.  $^{17}\text{O}$  NMR chemical shifts were referenced to  $\text{D}_2\text{O}$  at  $-2.7$  ppm (which corresponds to tap water at 0 ppm). The  $^{17}\text{O}$  nutation experiment was also recorded using  $\text{D}_2\text{O}$  at room temperature (with a natural abundance of  $^{17}\text{O}$ ).

The  $^2\text{H}$  NMR experiments performed on the PhoenixNMR probe were carried out using a solid echo pulse sequence with a  $\pi/2$  pulse length of 3.7  $\mu\text{s}$ .  $^2\text{H}$  MAS NMR experiments on D-TA\* were performed with a MAS frequency of 5 kHz and rotor-synchronised echo delay of one rotor period (200  $\mu\text{s}$ ), and spectra were acquired using 14,000 transients and recycle delay of 0.5 s. Static experiments were performed on D-IBU\*, using an echo delay of 30  $\mu\text{s}$ , and acquiring 122,500 transients with a recycle delay of 0.5 s.  $^2\text{H}$  chemical shifts were referenced to pure  $\text{D}_2\text{O}$  at 4.6 ppm. The  $^2\text{H}$  nutation experiment was also recorded using  $\text{D}_2\text{O}$  at room temperature.

The  $^1\text{H}$  nutation experiment was recorded using adamantane at room temperature with a MAS frequency of 10 kHz.

Variable temperature studies were carried out under static or magic-angle spinning conditions (spinning at 5 or 18 kHz). In each situation, the temperature was calibrated using  $\text{Pb}(\text{NO}_3)_2$ .<sup>[35]</sup> When working under MAS conditions, careful attention was paid to the setting of the magic angle using KBr ( $^{79}\text{Br}$  resonance). The accuracy of the magic-angle at each temperature of analysis could be verified on D-TA\*, by the absence of symmetric splitting of the  $^2\text{H}$  resonance and sidebands under magic angle spinning (see Figure S10). If judged necessary, the magic angle was carefully reset at the temperature of interest using KBr.

## 2.4 | Computational details

The NMR chemical shift calculations were performed within the density functional theory (DFT formalism using the QUANTUM-ESPRESSO (QE))<sup>[36]</sup> software. The PBE generalised gradient approximation<sup>[37]</sup> was used, and the valence electrons were described by norm-conserving pseudopotentials<sup>[38]</sup> in the Kleinman–Bylander form.<sup>[39]</sup> The wave functions were expanded on a plane wave basis set with kinetic energy cutoff of 80 Ry. The shielding tensor was computed using the Gauge Including Projector Augmented Wave (GIPAW)<sup>[40]</sup> approach, which permits the reproduction of the results of a fully converged all-electron calculation. Absolute shielding tensors are obtained. The isotropic chemical shift  $\delta_{\text{iso}}$  is defined as  $\delta_{\text{iso}} = -[\sigma - \sigma^{\text{ref}}]$ , where  $\sigma$  is the isotropic shielding and  $\sigma^{\text{ref}}$  is the isotropic shielding of the same nucleus in a reference system as previously described.<sup>[11]</sup> The principal components  $V_{xx}$ ,  $V_{yy}$  and  $V_{zz}$  of the electric field gradient (EFG) tensor are obtained by diagonalisation of the tensor. The quadrupolar interaction can then be characterised by the quadrupolar coupling constant  $C_Q$  and the asymmetry parameter  $\eta_Q$ , which are defined as  $C_Q = eQV_{zz}/h$  and  $\eta_Q = (V_{yy} - V_{xx})/V_{zz}$ . The experimental values of the quadrupole moments

of  $^{17}\text{O}$  ( $Q = -25.58 \times 10^{-30} \text{ m}^2$ ) and  $^2\text{H}$  ( $Q = +2.86 \times 10^{-30} \text{ m}^2$ )<sup>[41]</sup> were used to calculate  $C_Q$ .

Two crystallographic structures of racemic ibuprofen (CCDC 1041383 and 128796) were tested as starting points. The geometry optimisation of all atomic positions (keeping cell parameters fixed to experimental values) was performed for both low- and high-energy tautomers using the VASP code<sup>[42]</sup> and a Monkhorst–Pack k-space grid size of  $2 \times 3 \times 2$ . NMR parameters were then calculated keeping the relaxed atomic positions.

For the evaluation of the rotational barrier energy of the H-bonded  $(-\text{COOH})_2$  dimeric unit in ibuprofen, the crystalline structure # CCDC 128796 was used as a starting point (because the ibuprofen dimer is at the centre of the unit cell, thereby facilitating the application of a geometrical torsion). The dihedral angle  $C_{\text{ar}}-C_{(\text{H})}-C-\text{O}$  was varied and constrained, while the geometry of the rest of the molecule was optimised, and the energy subsequently calculated.

AIMD (Ab initio Molecular Dynamics) simulations were carried out with the CP2K code<sup>[43]</sup> consisting in the Born–Oppenheimer MD (BOMD) with PBE electronic representation, including the Grimme (D3) correction for dispersion,<sup>[44]</sup> GTH pseudopotentials,<sup>[45]</sup> combined plane wave, and triple-zeta valence with polarization (TZVP) basis sets.<sup>[46]</sup> The BOMD was performed using the NVT ensemble. The Nose–Hoover thermostat was used to control the average temperature at 300 K. Trajectories were accumulated over  $\sim 20$  ps with a time step of 0.5 fs.  $^2\text{H}$  and  $^{17}\text{O}$  NMR calculations were performed with QE every 400 steps, that is, every 200 fs.

## 3 | RESULTS

### 3.1 | Improved $^{17}\text{O}$ -enrichment protocols and preparation of doubly labelled molecules

Due to the very low natural abundance of  $^{17}\text{O}$  and  $^2\text{H}$  (Table 1), isotopic labelling is needed in order to be able to perform variable temperature solid-state NMR analyses in a reasonable time. While the deuteration of the carboxyl group can be easily achieved by exposure of the molecules to an excess of  $\text{D}_2\text{O}$ , the  $^{17}\text{O}$ -labelling of the carboxylic oxygen atoms is not as straightforward, notably due to the high cost of  $^{17}\text{O}$ -enriched water (1 ml of 90%  $^{17}\text{O}$ -enriched water can cost up to  $\sim 2000$  €). A previous study showed that terephthalic acid and ibuprofen could be enriched in  $^{17}\text{O}$  using mechanochemistry in a cost-efficient and user-friendly way.<sup>[11]</sup> However, our enrichment levels only averaged to  $\sim 3\%$ – $8\%$  per carboxylic oxygen for these molecules, which is  $\sim 2.5$  to 7 times less than the maximum

enrichment we could have expected based on the reactions and precursors involved. Hence, as part of this work, we first re-optimised the  $^{17}\text{O}$ -enrichment protocols for these two molecules.

The  $^{17}\text{O}$ -labelling procedure we have developed involves two ball-milling steps, which are performed back-to-back and followed by IR spectroscopy<sup>[11,47]</sup>: an activation of the carboxylic function using 1,1'-carbonyldiimidazole (CDI), followed by the hydrolysis of the acyl-imidazole intermediate using  $^{17}\text{O}$ -enriched water. If either of these steps is incomplete, the final enrichment level decreases. We retested the reaction conditions for TA and IBU using  $^{18}\text{O}$ -enriched water (due to its lower cost compared to  $^{17}\text{O}$ -enriched water) and found that longer milling times (30–60 min, instead of 5–10 min) were needed to ensure a better mixing of the reagents and full completion of activation and hydrolysis (see Figure S7 for illustrations in the case of IBU). We verified the reproducibility of the newly optimised enrichment protocols and then used them for the  $^{17}\text{O}$ -labelling of terephthalic acid and ibuprofen. In the case of terephthalic acid, the optimised  $^{17}\text{O}$ -enrichment protocol was applied to a deuterated form of the molecule (D-TA, fully deuterated on the aromatic cycle), while for ibuprofen, it was applied to the non-labelled form of the molecule. The average  $^{17}\text{O}$ -enrichment level per carboxylic oxygen achieved was  $\sim 20\%$  for D-TA\* (when using  $\sim 40\%$   $^{17}\text{O}$ -labelled water for the hydrolysis) and  $\sim 36\%$  for IBU\* (when using  $\sim 90\%$   $^{17}\text{O}$ -labelled water for the hydrolysis). The mass spectra of the  $^{17}\text{O}$ -labelled molecules can be found in the supporting information, together with other analyses that demonstrate the purity and crystallinity of the isolated molecules ( $^1\text{H}$  NMR,  $^{13}\text{C}$  NMR and powder X-ray diffraction) (see Figures S1–S6).

For ibuprofen, the  $^{17}\text{O}$ -enriched compound was then suspended in the presence of an excess of  $\text{D}_2\text{O}$  in order to exchange the carboxylic O–H group by O–D and form the doubly-labelled compound D-IBU\*. This reaction was followed by IR spectroscopy by looking at the O–H vibration modes' replacement by O–D ones (see Figure S8). It is worth noting that after completion of the reaction, the NMR rotor was immediately packed and stored under vacuum in the freezer to avoid back exchange of the carboxylic deuterium upon exposure to atmospheric humidity.

### 3.2 | Variable temperature $^{17}\text{O}$ MAS NMR of ibuprofen: Experiments and computational modelling

The  $^{17}\text{O}$  MAS NMR spectra of D-IBU\* were recorded at 14.1 T, while regulating the temperature between  $0^\circ\text{C}$

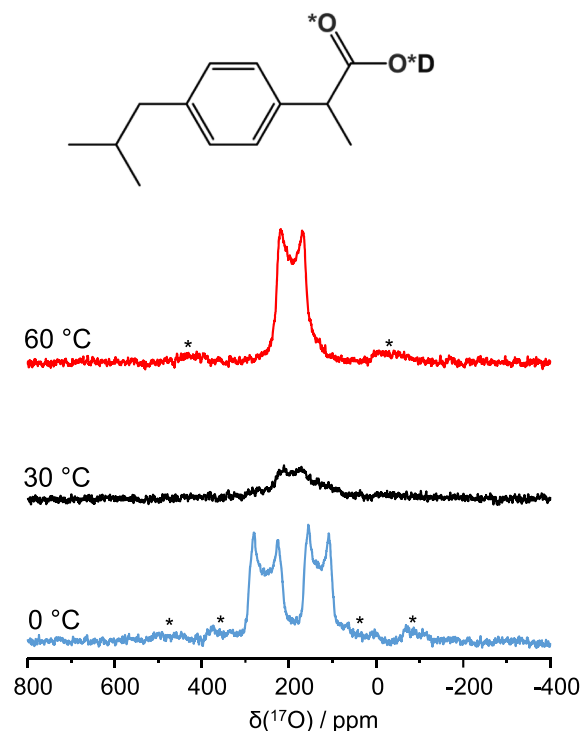


**FIGURE 1** Variable temperature  $^{17}\text{O}$  MAS NMR spectra of D-IBU\*. All  $^{17}\text{O}$  NMR spectra shown here were recorded using the same acquisition conditions (including the same number of scans). The temperatures indicated correspond to the sample temperature inside the rotor at each spinning speed, as determined from calibrations using  $\text{Pb}(\text{NO}_3)_2$ . Tentative fits of the  $0^\circ\text{C}$  and  $60^\circ\text{C}$  spectra can be found in supporting information (Figure S11). « \* » symbols correspond to spinning sidebands

and  $+60^\circ\text{C}$  (Figure 1). The  $^{17}\text{O}$  spectra show two second-order quadrupolar lineshapes at  $0^\circ\text{C}$ , which correspond to the C=O and C–OH groups. These signals progressively merge as the temperature is increased, leading to a single resonance with a characteristic second-order quadrupolar lineshape at  $60^\circ\text{C}$ . A similar observation had been made in our previous  $^{17}\text{O}$  NMR study of non-deuterated ibuprofen.<sup>[11]</sup> Fits of the spectra recorded at  $0^\circ\text{C}$  and  $60^\circ\text{C}$  can be found in supporting information (Figure S11). The fitted parameters at  $0^\circ\text{C}$  (i.e.,  $\delta_{\text{iso}} = 308 \pm 2$  ppm and  $|C_Q| = 7.9 \pm 0.1$  MHz for the C=O, and with  $\delta_{\text{iso}} = 179 \pm 2$  ppm and  $|C_Q| = 7.3 \pm 0.1$  MHz for the C–OH) were in line with those reported previously for non-deuterated ibuprofen, and with results from GIPAW-DFT calculations on the crystal structure.<sup>[11]</sup> A tentative fit of the data recorded at  $60^\circ\text{C}$  was also performed, resulting in intermediate  $\delta_{\text{iso}}$  and  $|C_Q|$  values ( $\delta_{\text{iso}} = 244 \pm 2$  ppm and  $|C_Q| = 7.6 \pm 0.1$  MHz).

Although several polymorphs of racemic ibuprofen have been reported,<sup>[48]</sup> the most stable form was obtained here, for which no polymorphic change is expected over the temperature range investigated by NMR. The changes

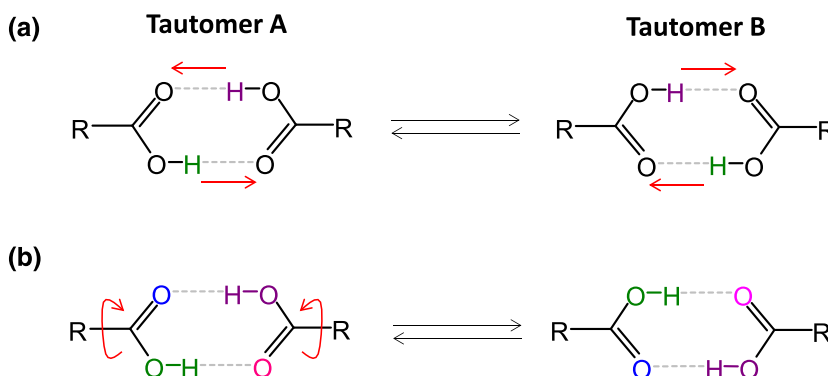
in  $^{17}\text{O}$  solid-state NMR spectra around room temperature could, however, be due to (i) variations in the relative populations of the two tautomeric forms undergoing double proton jumps (Scheme 2a),<sup>[24]</sup> and/or (ii)  $180^\circ$  flips of the  $(-\text{COOH})_2$  units (Scheme 2b),<sup>[49]</sup> the latter motion having been suggested to exist for ibuprofen by Geppi and co-workers.<sup>[50]</sup> Both of these motions were further analysed, using additional computational simulations to help rationalise the observations made by  $^{17}\text{O}$  NMR.

First, the possible influence of concerted double proton jumps between the two tautomeric forms of ibuprofen on the  $^{17}\text{O}$  MAS NMR data was looked into. Based on Wu and co-workers' recent work on a series of molecular crystals involving H-bonded carboxylic dimers, these motions can result in changes in  $^{17}\text{O}$  NMR spectra with temperature, depending on the relative population of the tautomeric forms.<sup>[24]</sup> Such proton exchanges occur on the ps timescale and can participate in the averaging of  $^{17}\text{O}$  NMR parameters between the two tautomeric forms. Here, a molecular dynamics simulation of racemic ibuprofen at 300 K was performed over a duration of 20 ps. This simulation brings evidence of the concerted double proton jumps and shows the evolution of the calculated average  $^{17}\text{O}$  NMR parameters of each oxygen (Figure 2), which appear to all progressively evolve towards averaged values. Nevertheless, a full averaging of the  $^{17}\text{O}$  NMR parameters could not be reached within the 20 ps timescale studied here.

For concerted double-proton jumps, the extent of averaging of the NMR parameters between both tautomers depends on the energy difference between the two forms and the analysis temperature.<sup>[24]</sup> In the case of racemic ibuprofen, Kolesov et al. reported an energy difference between both tautomers  $\sim 7.7 \text{ kJ mol}^{-1}$ , based on Raman spectroscopy measurements.<sup>[51]</sup> In our case, starting from the crystalline structure of racemic ibuprofen,<sup>[52]</sup> the energy difference between the tautomeric forms was calculated by DFT, yielding a value  $\sim 8.8 \text{ kJ mol}^{-1}$ , which is of the same order of magnitude as the experimental value of Kolesov. A similar energy

difference was found when performing calculations on structures in which the initial OH positions before geometry relaxation were varied, when starting from different crystallographic files (corresponding to neutron or X-ray data), and when modifying the dispersion energy parameters in VASP. Using these energy differences and the DFT-calculated  $^{17}\text{O}$  NMR parameters of each tautomer (Figure 3a), an approach similar to the one recently described by Wu and co-workers was then applied,<sup>[24]</sup> in order to see how the  $^{17}\text{O}$  NMR parameters may vary with temperature (Figure 3b). The most significant variations were observed for the isotropic chemical shifts. Yet, based on these calculations, a change of less than 10 ppm would have been expected for the « C=O » and « C-OH »-like resonances over the temperature range studied here (green-shaded region, Figure 3b), regardless of the energy difference chosen ( $8.8$  or  $7.7 \text{ kJ mol}^{-1}$ ). Similar conclusions would also have been expected for deuterated ibuprofen, for which an intermediate energy difference  $\sim 6.7 \text{ kJ mol}^{-1}$  between the two tautomeric forms has been derived from Raman spectroscopy analyses.<sup>[51]</sup> Overall, this implies that no merging of the two  $^{17}\text{O}$  signals as observed in Figure 1 would have been expected to arise from concerted double  $^1\text{H}$ -jumps only, on the basis of the calculated  $^{17}\text{O}$  NMR parameters of the two tautomers and their energy difference.

The motion related to a concerted rotation of the  $(-\text{COOH})_2$  group was then looked into. As mentioned above, the presence of this  $180^\circ$  flip had already been proposed in racemic ibuprofen on the basis of comprehensive  $^1\text{H}$  and  $^{13}\text{C}$  NMR analyses.<sup>[50]</sup> Moreover, it is worth noting that the observations of the evolution of the variable temperature  $^{17}\text{O}$  MAS NMR spectra of ibuprofen recall those reported by Wu and co-workers for nicotinic acid, in which the  $180^\circ$  rotation of an H-bonded  $-\text{COOH}$  unit was studied between  $\sim -20^\circ\text{C}$  and  $100^\circ\text{C}$  (although in the latter case, it is a single  $-\text{COOH}$  moiety H-bonded to N which undergoes the  $180^\circ$  flip).<sup>[22]</sup> Here, in contrast to the double proton jumps, the  $180^\circ$  flip motions in ibuprofen could not be made evident by molecular dynamics



**SCHEME 2** Illustration of dynamics that can occur between H-bonded carboxylic acids, leading to interconversion between the two tautomeric forms: (a) concerted double proton jump and (b) concerted  $180^\circ$  flips of the H-bonded  $(-\text{COOH})_2$  units



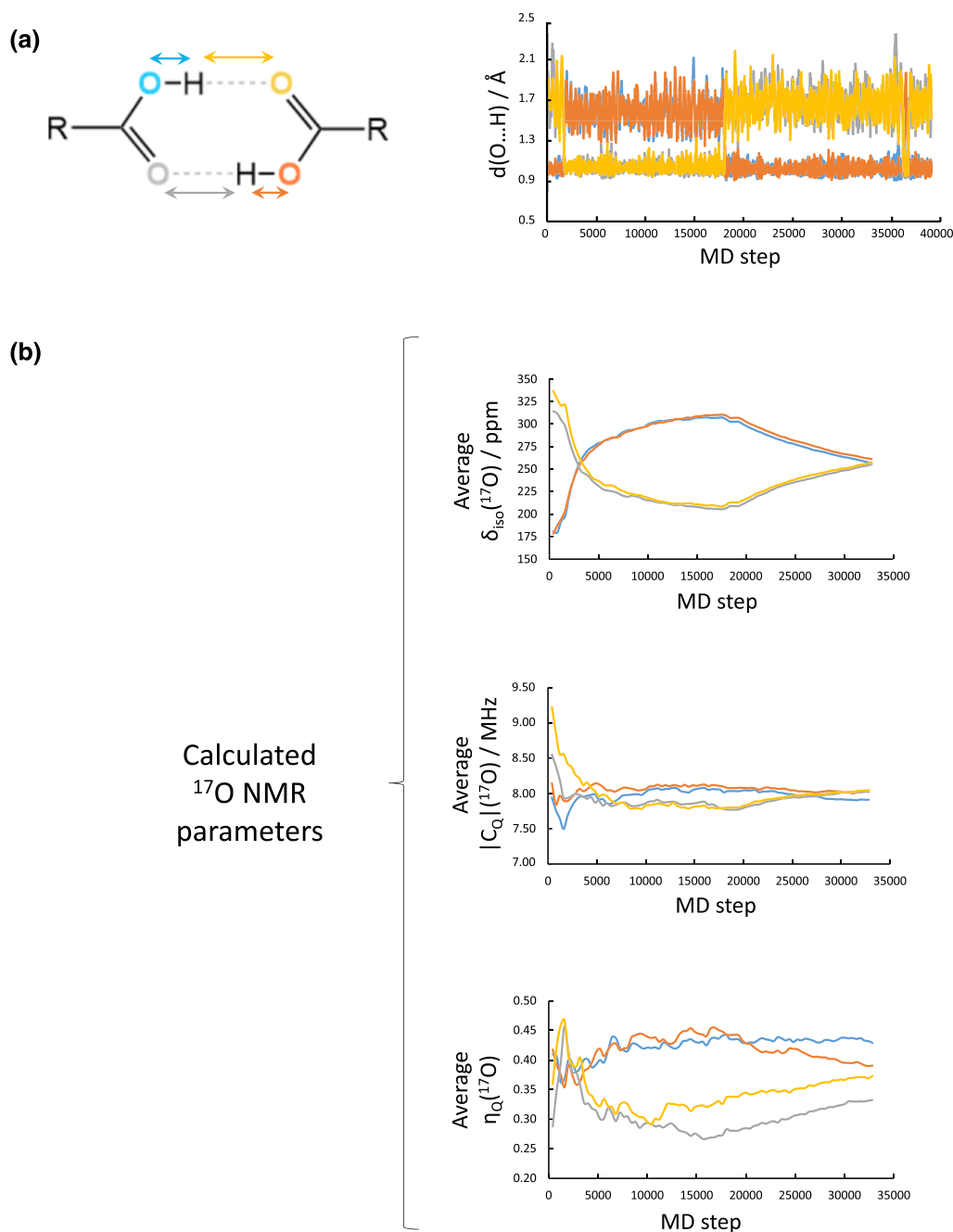


**FIGURE 2** Molecular dynamics simulation of the structure of racemic ibuprofen, performed at 300 K, for a duration of 20 ps, with steps of 0.5 fs, with a focus on calculated  $^{17}\text{O}$  NMR data. (a) Evolution of the H...O bond distances (in Å) in the dimer of the unit cell for which a concerted double  $^1\text{H}$  jump was observed over the timescale of the calculation performed here (for the other dimer, no jump was observed). (b) Evolution of the DFT-calculated averaged  $^{17}\text{O}$  NMR parameters for each oxygen site in this dimer (NMR parameters were calculated every 400 steps, i.e., every 200 fs; and for each new point calculated along the MD, the new value was averaged with the previous ones)

simulation due to the « short » timescale of our MD calculations. Nevertheless, the activation energy associated with this motion was evaluated by DFT, using an approach similar to the one proposed by Wu and co-workers for nicotinic acid.<sup>[22]</sup> More specifically, starting from the published structure of racemic ibuprofen, the  $(-\text{COOH})_2$  dimeric fragment was rotated (keeping all

other atomic positions constant), and the energy difference for each torsion angle was then calculated after the relaxation of all atomic positions (except for those defining the dihedral angle). Some of the calculated geometries are shown in Figure 4. In doing so, it was found that the energy barrier is  $\sim 75\text{--}100 \text{ kJ mol}^{-1}$  (the value depending on the direction chosen for the rotation

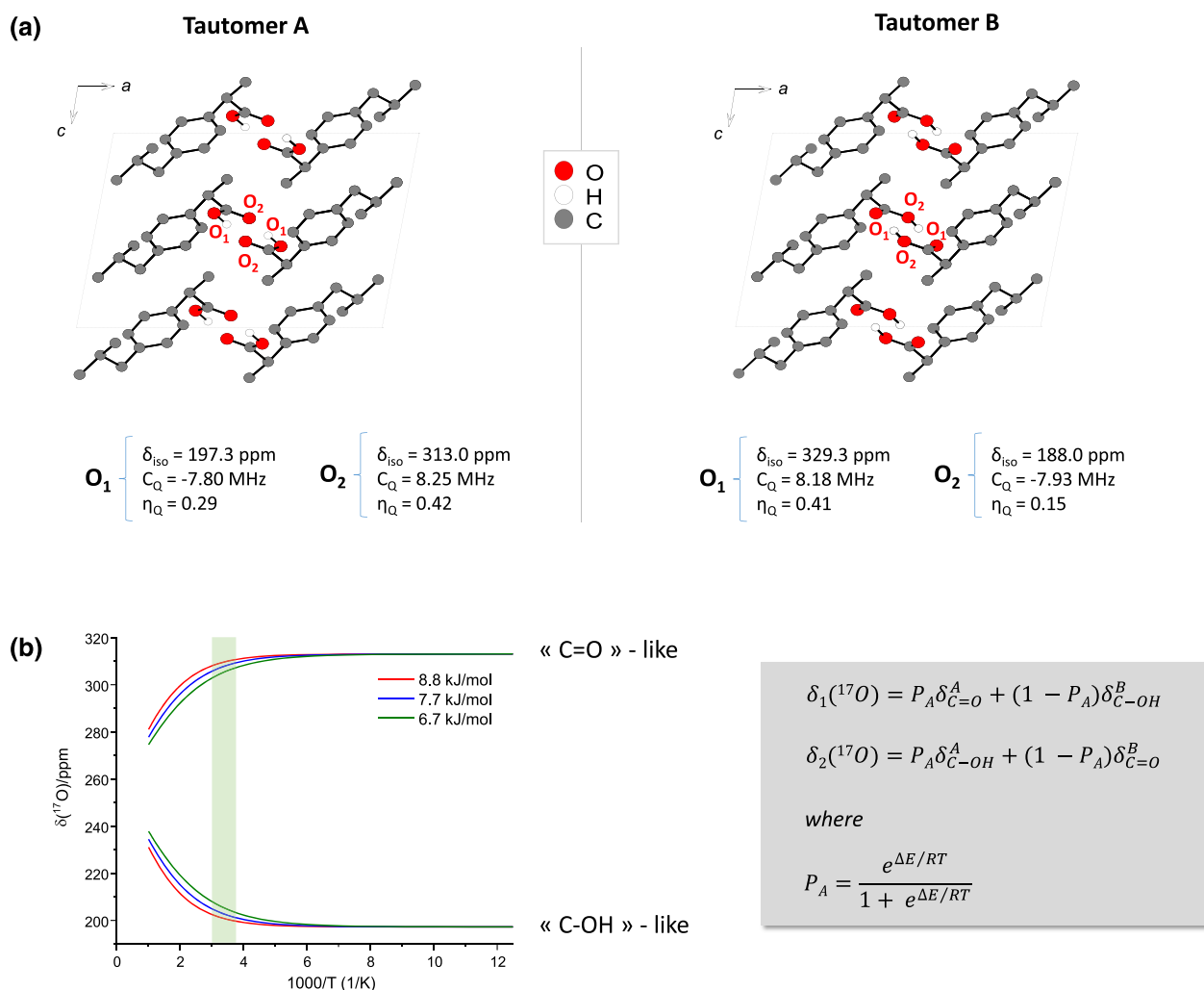


**FIGURE 3** (a) Representation of the two tautomeric forms of ibuprofen and their DFT-calculated  $^{17}\text{O}$  NMR parameters (for the  $(-\text{COOH})_2$  dimer) (not all atoms in the unit cell are shown here for clarity). (b) Temperature dependency of the  $^{17}\text{O}$  isotropic chemical shifts of the two tautomeric forms, for  $\Delta E$  values of 8.8 kJ mol $^{-1}$  (as calculated here by DFT for protonated ibuprofen) and of 7.7 and 6.7 kJ mol $^{-1}$  (as determined experimentally by Raman for protonated and deuterated ibuprofen, respectively).<sup>[51]</sup> The region shaded in green corresponds to the temperature range studied here by  $^{17}\text{O}$  NMR (i.e., between 0°C and 60°C). The equations used for the plot are recalled in the grey-shaded box<sup>[24]</sup> (in which the DFT-calculated values of  $\delta_{\text{C=O}}$  and  $\delta_{\text{C-OH}}$  of the two tautomeric forms given just above (Figure 3a) were used)

of the  $(-\text{COOH})_2$  unit). These values are very different from the one reported by Geppi on the basis of  $^1\text{H}$  and  $^{13}\text{C}$  NMR analyses, which had estimated the barrier to  $\sim 13$  kJ mol $^{-1}$ . However, they are still consistent with the energy barrier reported for  $(-\text{COOH})_2$  180° flips in other carboxylic dimers, for which values ranging from 50 to 85 kJ mol $^{-1}$  have been reported.<sup>[30,53]</sup> Part of the difference with the value reported by Geppi may come from the fact that computationally, we are probing the rotation of the carboxylic group by « freezing » the rest of the structure, while in the experimental study, other motions are occurring within the crystal structure,<sup>[50,54,55]</sup> which may indirectly facilitate the rotation of the carboxylic dimer. Overall, although the experimental and computational data shown here does not yet achieve a complete

picture of the  $(-\text{COOH})_2$  180° flip and double proton exchange processes occurring in racemic ibuprofen, it nevertheless demonstrates the added value of performing high-resolution  $^{17}\text{O}$  NMR analyses and computational simulations to try to help understand these movements.

### 3.3 | Variable temperature analyses using a $^1\text{H}$ - $^2\text{H}$ - $^{17}\text{O}$ tuning configuration

To complement the  $^{17}\text{O}$  MAS NMR study of the H-bonded carboxylic groups dynamics in D-IBU\*,  $^2\text{H}$  NMR experiments were carried out. Here, the possibility of performing  $^2\text{H}$  and  $^{17}\text{O}$  NMR analyses in a back-to-back fashion was investigated, using a diplexer connected to

Torsion angle (°)	Relative energy (kJ/mol)
3.9	0.0
26.4	13.6
52.2	57.3
57.3	63.3
75.1	93.2
95.6	83.5
107.4	81.3
125.3	62.2
174.4	7.3
272.6	100.1
304.1	45.7
328.2	11.2

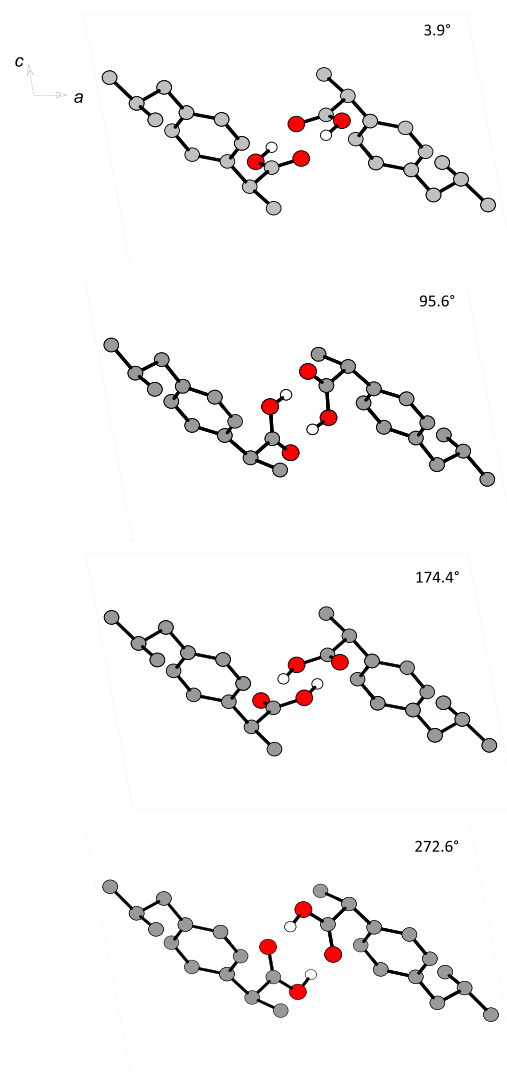


**FIGURE 4** DFT evaluation of the activation energy for the rotation of the  $(-\text{COOH})_2$  dimeric unit in crystalline racemic ibuprofen (using the CCDC crystal structure # 128796). Illustrations of some of the torsion angles are shown on the right (with C, O and H in grey, red and white, respectively; not all atoms in the unit cell are displayed here for clarity)

the probe for  $^1\text{H}$ - $^2\text{H}$ - $^{17}\text{O}$  tuning. Indeed, being able to analyse  $^2\text{H}$  and  $^{17}\text{O}$  local environments at any given temperature without changing the NMR probe configuration can be attractive, especially to avoid hysteresis effects that can occur upon heating or cooling some crystalline phases.

A schematic illustration of the mode of connection of the diplexer to the NMR probe is shown in Figure 5a, with further details being provided in the experimental section. The nutations obtained upon calibration of RF pulses using  $\text{D}_2\text{O}$  for  $^2\text{H}$  and  $^{17}\text{O}$ , and adamantane for  $^1\text{H}$ , are shown in Figure 5b. The loss in sensitivity of this triple resonance mode compared to the double resonance configuration was found to be reasonable (see Figure S12).

This probe configuration was first tested on the doubly labelled D-TA\* phase due to its higher weight

percentage in both  $^{17}\text{O}$  and  $^2\text{H}$ . The  $^2\text{H}$  and  $^{17}\text{O}$  MAS NMR spectra were recorded between  $-30^\circ\text{C}$  and  $+60^\circ\text{C}$  (Figure 6). No significant changes were observed in the  $^2\text{H}$  NMR. Although  $^2\text{H}$  relaxation measurements may have led to observable differences, these were not performed at this stage.

In the case of  $^{17}\text{O}$  NMR, only subtle variations with temperature were observed. A tentative deconvolution of the spectra is shown in Figure S13 (supporting information), considering the presence of 2 resonances corresponding to « C=O » and « C-OH » like environments, in agreement with the previous  $^{17}\text{O}$  NMR work reported for non-deuterated terephthalic acid.<sup>[11]</sup> Due to the overlap of both resonances, MQMAS experiments at each temperature of analysis (or variable temperature analyses at a second magnetic field) would have been needed to confirm the fitted parameters. Nevertheless,

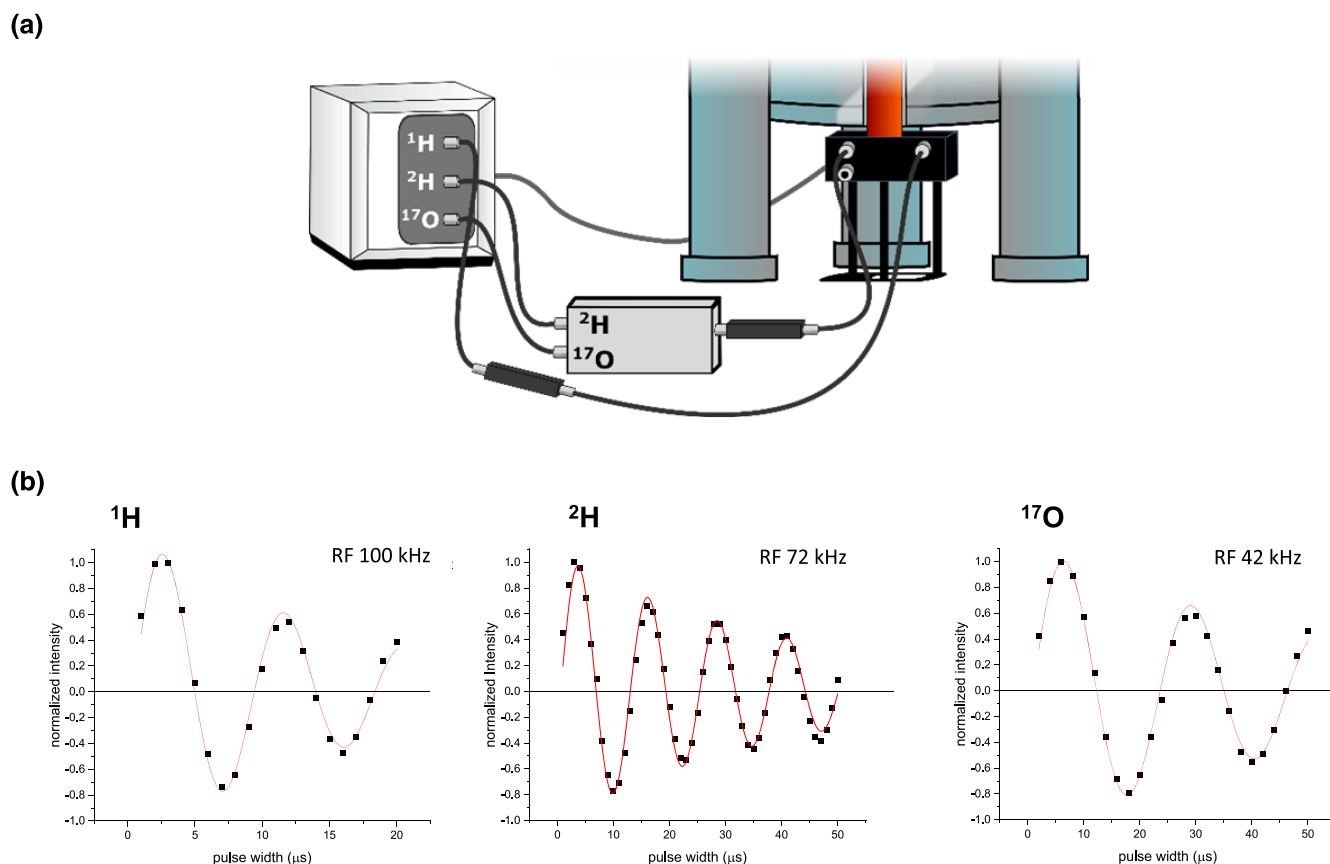
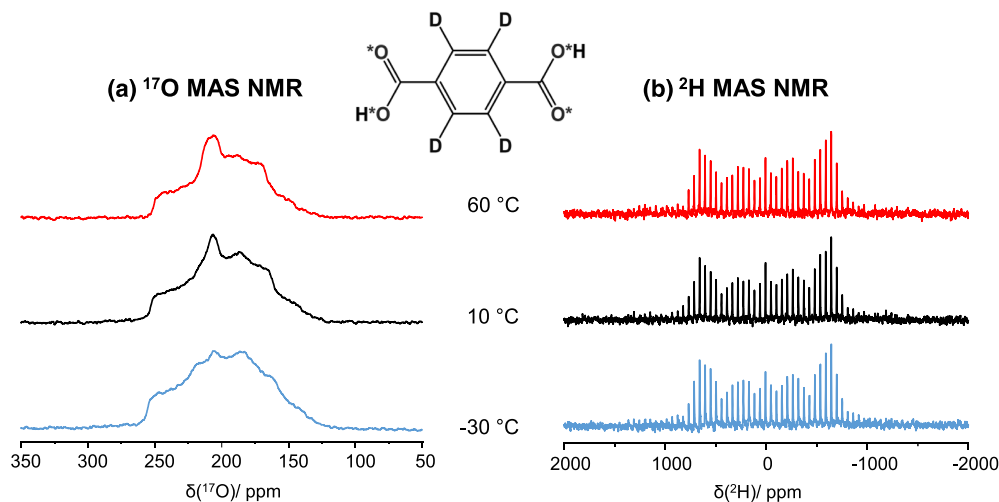


**FIGURE 5** (a) Schematic representation of the connection mode of the diplexer to the NMR probe and (b) nutations achieved on the  $^1\text{H}$ ,  $^2\text{H}$  and  $^{17}\text{O}$  channels in triple resonance mode. The  $810^\circ/90^\circ$  intensity ratio determined here for  $^2\text{H}$  is 0.51

**FIGURE 6** Variable temperature  $^{17}\text{O}$  and  $^2\text{H}$  NMR spectra of D-TA\*, recorded under magic angle spinning conditions. The temperatures indicated correspond to the sample temperature inside the rotor, as determined from calibrations at different MAS speeds using  $\text{Pb}(\text{NO}_3)_2$



the small variations observed for D-TA\* over this temperature range may reflect effects of H-bonding tautomerism and/or polymorphic changes of terephthalic acid.<sup>[56–62]</sup> Indeed, on the one hand, previous studies in the literature have shown that the H-bonded carboxylic protons of terephthalic acid are dynamically disordered at room

temperature, undergoing concerted double-proton jumps (Scheme 2a).<sup>[56,61,63]</sup> The fact that the free enthalpy difference between both tautomeric forms has been estimated experimentally to only  $\sim 2 \text{ kJ mol}^{-1}$  for terephthalic acid<sup>[61]</sup> implies that small changes should be observable over the temperature range studied here

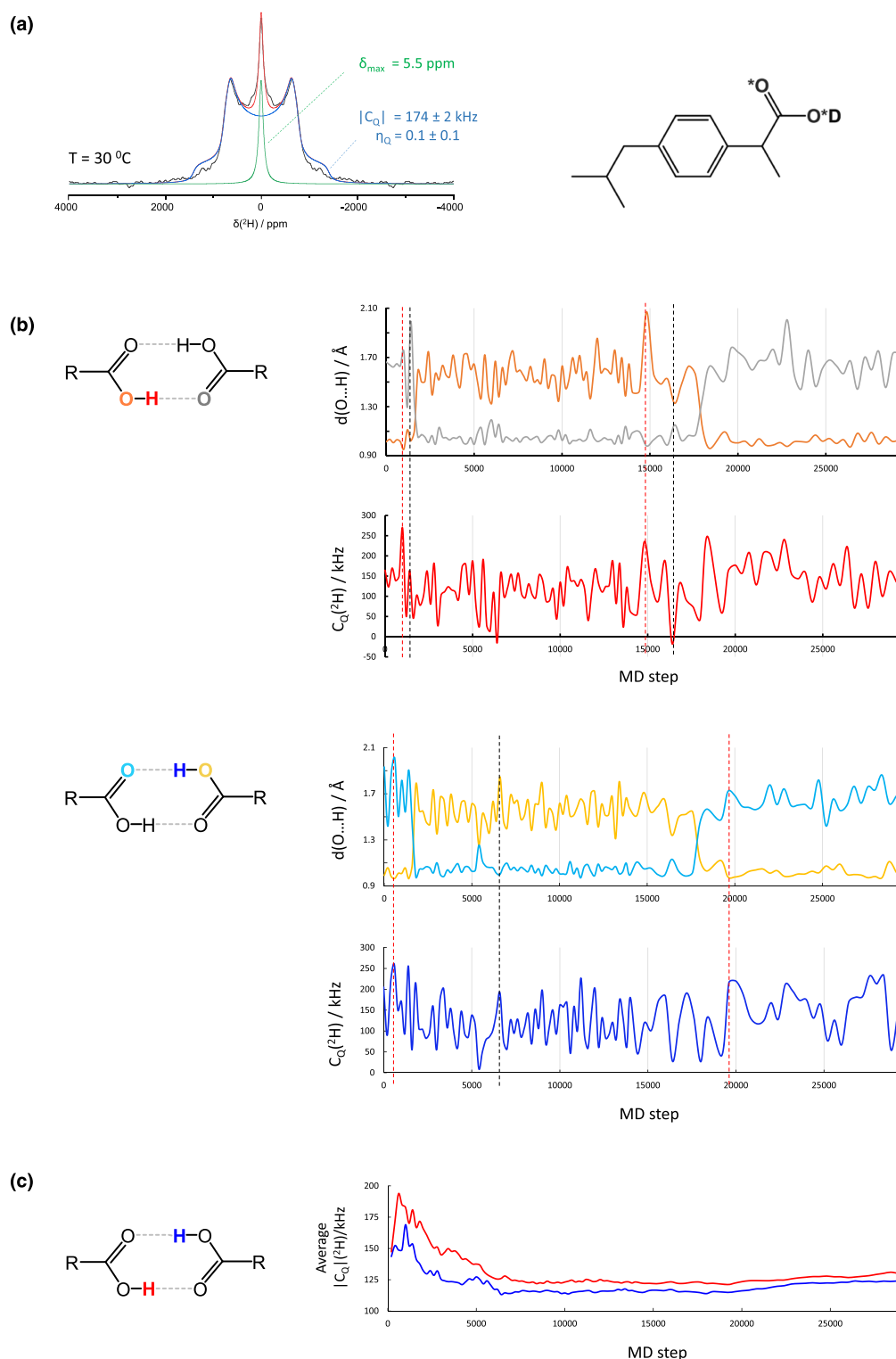


**FIGURE 7** (a) Fit of the experimental static  $^2\text{H}$  NMR spectrum of D-IBU\* at  $30^\circ\text{C}$ , after symmetrisation of the  $^2\text{H}$  lineshape (experimental spectrum in black, and its fit in red, considering two contributions, with in blue the H-bonded  $-(\text{COOD})_2$  dimeric unit of D-IBU\*, and in green the sharp mobile species). (b) Molecular dynamics simulation of the structure of racemic ibuprofen, performed at  $300\text{ K}$ , with steps of  $0.5\text{ fs}$  (shown here over duration of  $\sim 15\text{ ps}$ ), with a focus on calculated  $^2\text{H}$  NMR data. Evolution of the H $\cdots$ O bond distances (in  $\text{\AA}$ ) in the dimer of the unit cell for which a concerted double proton jump was observed over the timescale of the calculation, and evolution of the « instantaneous » DFT-calculated  $^2\text{H}$  quadrupolar coupling constant  $C_Q$  for this dimer (NMR parameters calculations were performed as a first approximation from the MD structures of protonated ibuprofen, every 200 steps, up to step # 14000, and then every 400 steps). (c) Evolution of the average calculated  $|C_Q|$  values along with the MD timescale, showing that the  $^2\text{H}$   $|C_Q|$  converges towards an average value

(because this value is of the same order of magnitude as those reported for cinnamic acid and aspirin).<sup>[24]</sup>

On the other hand, the variations in the  $^{17}\text{O}$  MAS NMR spectra may also reflect the existence of several polymorphic forms of terephthalic acid. Out of the three polymorphs reported to date for this molecule, triclinic forms (I) and (II) have been the object of much attention.<sup>[57–60,62,64]</sup> Both consist of chains of terephthalic acid molecules, in which each molecule is hydrogen-bonded to two others through carboxylic acid dimer motifs. These chains are further assembled into 2D layers, which pack differently from one polymorph to the other. Moreover, when looking at the terephthalic acid motif itself, slightly different dihedral angles are found between the carboxylic function and the aromatic cycle when both polymorphs are compared.<sup>[62]</sup> Although both forms can be observed under ambient temperature and pressure, form (I) appears to be the least stable. Its transformation into form (II) has been studied both experimentally and computationally.<sup>[57,58,60]</sup> More specifically, this transformation was found to occur above 70°C, to be sensitive to pressure and to be caused by a « surface-mediated nucleation » type of process, triggered by the movement of the supramolecular chains of terephthalic acid at the surface of the crystallites.<sup>[58–60]</sup> In our case, given that D-TA\* was obtained here as polymorph (I) (see Figure S1), it is possible that the subtle modifications in the  $^{17}\text{O}$  NMR spectra upon heating are indicative of the onset of transformation into form (II), caused by the increase in temperature and possibly also pressure (due to the spinning). More specifically,  $^{17}\text{O}$  NMR may indicate that changes in the local environment of the carboxylic functions precede more significant movements of the supramolecular chains. Although the observations made in  $^{17}\text{O}$  NMR for D-TA\* were not further investigated at this stage, they point to the interest of analysing molecular crystals by this technique, notably to help understand polymorphic transformations.

Using this  $^2\text{H}$ – $^{17}\text{O}$  probe configuration, preliminary  $^2\text{H}$  NMR studies were also performed in the case of D-IBU\*. The static  $^2\text{H}$  NMR spectra revealed the presence of two main resonances (Figure 7a): one broad signal with a characteristic deuterium quadrupolar lineshape and a much sharper signal at the centre of the spectrum, the relative intensity of which was found to increase with temperature, under the measurement conditions used here (Figure S14). The fitting of the broad  $^2\text{H}$  NMR signal at each temperature was performed, yielding similar quadrupolar parameters between 0°C and 60°C, with  $|C_Q| \sim 170$  kHz and  $\eta_Q \sim 0.1$  (Figure S14). These values are close to those reported previously for supercooled and glassy states of deuterated ibuprofen,<sup>[65]</sup> as well as for other crystal structures of organic molecules involving H-

bonded carboxylic dimers.<sup>[66]</sup> Hence, this  $^2\text{H}$  resonance is characteristic of  $(-\text{COOD})_2$  dimeric structures in crystalline D-IBU\*, with the  $^2\text{H}$  NMR parameters being averaged between the two interconverting tautomeric forms of ibuprofen. The MD simulations and DFT calculations of  $^2\text{H}$  NMR parameters associated with these double proton jumps are provided in Figure 7b,c. In agreement with previous observations made by Schmidt and Sebastiani<sup>[32]</sup> for H-bonded carboxylic acids, these calculations show that the « instantaneous »  $C_Q$  values tend to follow the evolution of the longer  $\text{O} \cdots \text{H}$  distance (Figure 7b, dashed vertical lines).

The sharp central  $^2\text{H}$  NMR resonance, on the other hand, is very weak at 0°C, where it is centred at 5.2 ppm. At 60°C, it becomes increasingly sharp and intense and shifts to 9.4 ppm. Based on the observed chemical shifts and the  $^2\text{H}$  NMR measurements also performed on melted D-IBU\* (see Figure S9), this resonance appears to arise from different species: it is consistent with a small amount of residual liquid (mobile) water at  $\sim 0^\circ\text{C}$ , and to the predominant presence of highly mobile ibuprofen at 60°C (in a melt-like state, the melting temperature of ibuprofen being  $\sim 75^\circ\text{C}$ ). It is worth noting that in comparison to previous variable temperature  $^2\text{H}$  NMR studies on supercooled and glassy ibuprofen,<sup>[65]</sup> the fully motionally narrowed  $^2\text{H}$  NMR signal is observed here at a higher temperature (80°C in Figure S9, vs. 36°C in the work by Bauer et al.<sup>[65]</sup>). Overall, it is clear that  $^2\text{H}$  and  $^{17}\text{O}$  NMR spectra provide complementary information regarding the dynamics occurring around the carboxylic groups in racemic ibuprofen. It can be hypothesised that the progressive increase in mobility within ibuprofen crystals with temperature (especially around the carboxylic function) allows some molecules to behave as in a melt-like state, which may favour dynamics like the 180°  $(-\text{COOH})_2$  flip to occur with energy barriers lower than the ones calculated by DFT, thereby explaining the observations made by  $^{17}\text{O}$  NMR. However, more extensive investigations would be needed to confirm this.

## 4 | CONCLUSION

In this article, three different aspects related to the structural analysis of molecular crystals containing carboxylic functions have been looked into. First, improved  $^{17}\text{O}$  labelling protocols based on mechanochemistry have been developed. This has allowed average enrichment levels exceeding 20% in  $^{17}\text{O}$  per carboxylic oxygen to be reached for two key molecules: (i) ibuprofen, a non-steroidal anti-inflammatory drug, which is seen as a « golden standard » for numerous investigations in pharmaceutical sciences aiming at improving drug

formulations, and (ii) terephthalic acid, which is one of the most commonly used ligands for the design of metal-organic frameworks (MOFs). In the latter case, the  $^{17}\text{O}$  labelling was performed here on a deuterated version of the terephthalic acid precursor (with deuteration on the aromatic ring), thereby leading to the formation of a doubly labelled molecule, which would be of key interest for studying the structure and reactivity or a variety of MOFs, including the most complex ones. Such ligands should enable studying both the dynamics related to the  $180^\circ$  flips of the aromatic ring (using  $^2\text{H}$  NMR) and the binding properties to metal cations in a given system (using  $^{17}\text{O}$  NMR).

Second, the experimental and computational study of  $^{17}\text{O}$  and  $^2\text{H}$  enriched ibuprofen has shed light on the interest in looking at both of these nuclei when studying the dynamics occurring around the carboxylic groups. Although further investigations would be needed to fully understand the experimental observations, this work nevertheless complements previous studies on racemic ibuprofen crystals involving  $^1\text{H}$  and  $^{13}\text{C}$  NMR, by underscoring the complexity of the molecular motions around the carboxylic functions. More generally, this study shows how the NMR study of quadrupolar nuclei like  $^{17}\text{O}$  and  $^2\text{H}$  may provide new opportunities for investigating polymorphic transitions of ibuprofen,<sup>[67]</sup> as well as its confined or « supercooled » states.<sup>[65,68,69]</sup> Indeed, the polarity and H-bonding capability of carboxylic functions imply that these are often key to interactions between molecules and with materials surfaces, meaning that direct insight into the local environment of the carboxylic atoms (among which oxygen) is important for detailed structure characterization purposes.

Lastly, we have presented some of the possibilities provided by combining  $^2\text{H}$ - $^{17}\text{O}$  diplexers to NMR probes for studying by NMR the  $^2\text{H}$  and  $^{17}\text{O}$  nuclei at any given temperature, without having to change probe configurations. The RF performance of the probe used along with the diplexer was shown to be suitable for such applications, as illustrated for both terephthalic acid and ibuprofen. While the experiments shown here were mainly performed in a back-to-back fashion, we will look into recording them using « double receiver » setups in future studies. Moreover, beyond these possibilities, the next step will consist of using such hardware configurations to perform multi-channel  $^2\text{H}$  and  $^{17}\text{O}$  correlation experiments. This pair of nuclear spins has not yet been studied due to the very similar Larmor frequencies of the two isotopes but could offer new opportunities for helping understand further the structure of a variety of molecular and materials systems, considering that H and O are two atoms, which are very often present. This is a point we will be looking into in the near future. Such

instrumental developments will add to the ongoing effort to broaden the scope of heteronuclear correlations accessible to NMR spectroscopists with spin pairs of similar Larmor frequencies (e.g.,  $^{13}\text{C}$ - $^{27}\text{Al}$ ,<sup>[70,71]</sup>  $^{13}\text{C}$ - $^{45}\text{Sc}$ ,<sup>[71]</sup>  $^{13}\text{C}$ - $^{81}\text{Br}$  ...<sup>[72]</sup>).

## ACKNOWLEDGEMENTS

This project has received funding from the European Research Council (ERC) under the European Union's Horizon 2020 research and innovation programme (grant agreement No 772204; 2017 ERC-COG, MISOTOP project). NMR spectroscopic calculations were performed using HPC resources from GENCI-IDRIS (Grant 097535). Powder X-ray diffraction, mass spectrometry and solution NMR characterizations were performed with the support of the local Balard Plateforme d'Analyses et de Caractérisation (PAC Balard).

## ORCID

Chia-Hsin Chen  <https://orcid.org/0000-0001-5151-1765>

Ieva Goldberga  <https://orcid.org/0000-0003-4284-3527>

Sébastien Mittele  <https://orcid.org/0000-0003-2471-1088>

Jessica Špačková  <https://orcid.org/0000-0001-6255-8788>

Thomas-Xavier Métro  <https://orcid.org/0000-0003-2280-3595>

Bruno Alonso  <https://orcid.org/0000-0002-3430-1931>

Christel Gervais  <https://orcid.org/0000-0001-7450-1738>

Danielle Laurencin  <https://orcid.org/0000-0002-7445-0528>

## REFERENCES

- [1] Z. Gan, I. Hung, X. Wang, J. Paulino, G. Wu, I. M. Litvak, P. L. Gor'kov, W. W. Brey, P. Lendi, J. L. Schiano, M. D. Bird, I. R. Dixon, J. Toth, G. S. Boebinger, T. A. Cross, *J. Magn. Reson.* **2017**, *284*, 125.
- [2] Y. Ishii, A. Wickramasinghe, I. Matsuda, Y. Endo, Y. Ishii, Y. Nishiyama, T. Nemoto, T. Kamihara, *J. Magn. Reson.* **2018**, *286*, 99.
- [3] S. Penzel, A. Oss, M.-L. Org, A. Samoson, A. Böckmann, M. Ernst, B. H. Meier, *J. Biomol. NMR* **2019**, *73*(1), 19.
- [4] A. V. Wijesekara, A. Venkatesh, B. J. Lampkin, B. VanVeller, J. W. Lubach, K. Nagapudi, I. Hung, P. L. Gor'kov, Z. Gan, A. J. Rossini, *Chem-Eur J.* **2020**, *26*(35), 7881.
- [5] R. Zhang, K. H. Mroue, A. Ramamoorthy, *Acc. Chem. Res.* **2017**, *50*(4), 1105.
- [6] K. J. Sanders, A. J. Pell, S. Wegner, C. P. Grey, G. Pintacuda, *Chem. Phys. Lett.* **2018**, *697*, 29.
- [7] F. A. Perras, A. Venkatesh, M. P. Hanrahan, T. W. Goh, W. Huang, A. J. Rossini, M. Pruski, *J. Magn. Reson.* **2017**, *276*, 95.
- [8] L. A. O'Dell, Ultra-wideline Solid-State NMR: Developments and Applications of the WCPMG Experiment, in *Modern*

- Magnetic Resonance*, (Ed: G. A. Webb), Springer International Publishing, Cham **2017**, pp. 1–22.
- [9] S. Gupta, R. Tycko, *J. Biomol. NMR* **2018**, *70*(2), 103.
- [10] V. W. C. Wong, D. G. Reid, W. Y. Chow, R. Rajan, M. Green, R. A. Brooks, M. J. Duer, *J. Biomol. NMR* **2015**, *63*(2), 119.
- [11] T.-X. Métro, C. Gervais, A. Martinez, C. Bonhomme, D. Laurencin, *Angew. Chem. Int. Ed. Engl.* **2017**, *56*(24), 6803.
- [12] M. A. Hope, B. Zhang, B. Zhu, D. M. Halat, J. L. MacManus-Driscoll, C. P. Grey, *Chem. Mater.* **2020**, *32*, 7921.
- [13] A. S. Lilly Thankamony, J. J. Wittmann, M. Kaushik, B. Corzilius, *Prog. Nucl. Magn. Reson. Spectrosc.* **2017**, *102–103*, 120.
- [14] R. W. Hooper, B. A. Klein, V. K. Michaelis, *Chem. Mater.* **2020**, *32*(11), 4425.
- [15] C. Leroy, D. L. Bryce, *Prog. Nucl. Magn. Reson. Spectrosc.* **2018**, *109*, 160.
- [16] D. L. Bryce, *Dalton Trans.* **2019**, *48*(23), 8014.
- [17] I. Matlahov, P. C. A. van der Wel, *Methods* **2018**, *148*, 123.
- [18] V. S. Mandala, J. K. Williams, M. Hong, *Annu. Rev. Biophys.* **2018**, *47*(1), 201.
- [19] J. V. Milić, J.-H. Im, D. J. Kubicki, A. Ummadisingu, J.-Y. Seo, Y. Li, M. A. Ruiz-Preciado, M. I. Dar, S. M. Zakeeruddin, L. Emsley, M. Grätzel, *Adv. En. Mater.* **2019**, *9*(20), 1900284.
- [20] M. T. Dunstan, D. M. Halat, M. L. Tate, I. R. Evans, C. P. Grey, *Chem. Mater.* **2019**, *31*(5), 1704.
- [21] Y.-X. Xiang, G. Zheng, G. Zhong, D. Wang, R. Fu, Y. Yang, *Solid State Ion.* **2018**, *318*, 19.
- [22] J. Lu, I. Hung, A. Brinkmann, Z. Gan, X. Kong, G. Wu, *Angew. Chem. Int. Ed. Engl.* **2017**, *56*(22), 6166.
- [23] G. Wu, *Prog. Nucl. Magn. Reson. Spectrosc.* **2019**, *114–115*, 135.
- [24] G. Wu, I. Hung, Z. Gan, V. Terskikh, X. Kong, *J. Phys. Chem. A* **2019**, *123*(38), 8243.
- [25] J. Catalano, A. Murphy, Y. Yao, N. Zumbulyadis, S. A. Centeno, C. Dybowski, *Solid State Nucl. Magn. Reson.* **2018**, *89*, 21.
- [26] D. I. Kolokolov, H. Jovic, A. G. Stepanov, V. Guillermin, T. Devic, C. Serre, G. Férey, *Angew. Chem. Int. Ed. Engl.* **2010**, *49*(28), 4791.
- [27] A. E. Khudozhitkov, D. I. Kolokolov, A. G. Stepanov, *J. Phys. Chem. C* **2018**, *122*(24), 12956.
- [28] X. Jiang, H.-B. Duan, M. J. Jellen, Y. Chen, T. S. Chung, Y. Liang, M. A. Garcia-Garibay, *J. Am. Chem. Soc.* **2019**, *141*(42), 16802.
- [29] Y. Dai, V. Terskikh, A. Brinkmann, G. Wu, *Cryst. Growth Des.* **2020**, *20*(11), 7484.
- [30] W. Scheubel, H. Zimmermann, U. Haeberlen, *J. Magn. Reson.* **1988**, *80*(3), 401.
- [31] X. Kong, M. Shan, V. Terskikh, I. Hung, Z. Gan, G. Wu, *J. Phys. Chem. B.* **2013**, *117*(33), 9643.
- [32] J. Schmidt, D. Sebastiani, *J. Chem. Phys.* **2005**, *123*(7), 074501.
- [33] T. Friščić, C. Mottillo, H. M. Titi, *Angew. Chem. Int. Ed. Engl.* **2019**, *59*, 1018.
- [34] P. Pyykkö, *Mol. Phys.* **2018**, *116*(10), 1328.
- [35] A. Bielecki, D. P. Burum, *J. Magn. Reson., Ser. A* **1995**, *116*(2), 215.
- [36] P. Giannozzi, S. Baroni, N. Bonini, M. Calandra, R. Car, C. Cavazzoni, D. Ceresoli, G. L. Chiarotti, M. Cococcioni, I. Dabo, A. Dal Corso, S. de Gironcoli, S. Fabris, G. Fratesi, R. Gebauer, U. Gerstmann, C. Gougousis, A. Kokalj, M. Lazzeri, L. Martin-Samos, N. Marzari, F. Mauri, R. Mazzarello, S. Paolini, A. Pasquarello, L. Paulatto, C. Sbraccia, S. Scandolo, G. Sclauzero, A. P. Seitsonen, A. Smogunov, P. Umari, R. M. Wentzcovitch, *J. Phys. Condens. Matter* **2009**, *21*(39), 395502.
- [37] J. P. Perdew, K. Burke, M. Ernzerhof, *Phys. Rev. Lett.* **1996**, *77*(18), 3865.
- [38] N. Troullier, J. L. Martins, *Phys. Rev. B* **1991**, *43*(3), 1993.
- [39] L. Kleinman, D. M. Bylander, *Phys. Rev. Lett.* **1982**, *48*(20), 1425.
- [40] C. J. Pickard, F. Mauri, *Phys. Rev. B* **2001**, *63*(24), 245101.
- [41] P. Pyykkö, *Mol. Phys.* **2008**, *106*(16–18), 1965.
- [42] J. Hafner, *J. Comput. Chem.* **2008**, *29*(13), 2044.
- [43] J. VandeVondele, M. Krack, F. Mohamed, M. Parrinello, T. Chassaing, J. Hutter, *Comput. Phys. Commun.* **2005**, *167*(2), 103.
- [44] S. Grimme, J. Antony, S. Ehrlich, H. Krieg, *J. Chem. Phys.* **2010**, *132*(15), 154104.
- [45] S. Goedecker, M. Teter, J. Hutter, *Phys. Rev. B* **1996**, *54*(3), 1703.
- [46] J. VandeVondele, J. Hutter, *J. Chem. Phys.* **2007**, *127*(11), 114105.
- [47] J. Špačková, C. Fabra, S. Mitteleite, E. Gaillard, C.-H. Chen, G. Cazals, A. Lebrun, S. Sene, D. Berthomieu, K. Chen, Z. Gan, C. Gervais, T.-X. Métro, D. Laurencin, *J. Am. Chem. Soc.* **2020**, *142*(50), 21068.
- [48] E. Dudognon, N. T. Correia, F. Danède, M. Descamps, *Pharm. Res.* **2013**, *30*(1), 81.
- [49] B. Filsinger, H. Zimmermann, U. Haeberlen, *Mol. Phys.* **1992**, *76*(1), 157.
- [50] E. Carignani, S. Borsacchi, M. Geppi, *ChemPhysChem* **2011**, *12*(5), 974.
- [51] A. G. Demkin, B. A. Kolesov, *J. Phys. Chem. A* **2019**, *123*(26), 5537.
- [52] K. Ostrowska, M. Kropidłowska, A. Katrusiak, *Cryst. Growth Des.* **2015**, *15*(3), 1512.
- [53] S. Idziak, *Mol. Phys.* **1989**, *68*(6), 1335.
- [54] E. Carignani, S. Borsacchi, A. Marini, B. Mennucci, M. Geppi, *J. Phys. Chem. C* **2011**, *115*(50), 25023.
- [55] M. Geppi, S. Guccione, G. Mollica, R. Pignatello, C. A. Veracini, *Pharm. Res.* **2005**, *22*(9), 1544.
- [56] B. A. Kolesov, *J. Phys. Chem. Solids* **2020**, *138*, 109288.
- [57] D. J. Goossens, E. J. Chan, *Acta Crystallogr. Sect. B* **2017**, *73*(1), 112.
- [58] G. T. Beckham, B. Peters, C. Starbuck, N. Variankaval, B. L. Trout, *J. Am. Chem. Soc.* **2007**, *129*(15), 4714.
- [59] M. Śledź, J. Janczak, R. Kubiak, *J. Mol. Struct.* **2001**, *595*(1), 77.
- [60] R. J. Davey, S. J. Maginn, S. J. Andrews, S. N. Black, A. M. Buckley, D. Cottier, P. Dempsey, R. Plowman, J. E. Rout, D. R. Stanley, A. Taylor, *J. Chem. Soc. Faraday Trans.* **1994**, *90*(7), 1003.
- [61] B. H. Meier, R. R. Ernst, *J. Solid State Chem.* **1986**, *61*(1), 126.
- [62] M. Bailey, C. J. Brown, *Acta Crystallogr.* **1967**, *22*(3), 387.
- [63] E. A. Pritchina, B. A. Kolesov, *Spectrosc. Acta A* **2018**, *202*, 319.
- [64] J. J. McKinnon, F. P. A. Fabbiani, M. A. Spackman, *Cryst. Growth Des.* **2007**, *7*(4), 755.
- [65] S. Bauer, M. Storek, C. Gainaru, H. Zimmermann, R. Böhmer, *J. Phys. Chem. B.* **2015**, *119*(15), 5087.
- [66] I. J. F. Poplett, J. A. S. Smith, *J. Chem. Soc., Faraday Trans. 2* **1981**, *77*(8), 1473.



- [67] E. Dudognon, F. Danède, M. Descamps, N. T. Correia, *Pharm. Res.* **2008**, 25(12), 2853.
- [68] K. Adrjanowicz, K. Kaminski, M. Dulski, P. Włodarczyk, G. Bartkowiak, L. Popenda, S. Jurga, J. Kujawski, J. Kruk, M. K. Bernard, M. Paluch, *J. Chem. Phys.* **2013**, 139(11), 111103.
- [69] F. Tielens, N. Folliet, L. Bondaz, S. Etemovic, F. Babonneau, C. Gervais, T. Azaïs, *J. Phys. Chem. C* **2017**, 121(32), 17339.
- [70] F. Pourpoint, J. Trébosc, R. M. Gauvin, Q. Wang, O. Lafon, F. Deng, J.-P. Amoureux, *ChemPhysChem* **2012**, 13(16), 3605.
- [71] L. van Wüllen, H. Koller, M. Kalwei, *Phys. Chem. Chem. Phys.* **2002**, 4(9), 1665.
- [72] M. Makrinich, M. Sambol, A. Goldbourn, *Phys. Chem. Chem. Phys.* **2020**, 22, 21022.

## SUPPORTING INFORMATION

Additional supporting information may be found online in the Supporting Information section at the end of this article.

**How to cite this article:** Chen C-H, Goldberga I, Gaveau P, et al. Looking into the dynamics of molecular crystals of ibuprofen and terephthalic acid using  $^{17}\text{O}$  and  $^2\text{H}$  nuclear magnetic resonance analyses. *Magn Reson Chem.* 2021;59:975–990. <https://doi.org/10.1002/mrc.5141>